M. H. Sanad*, Fawzy A. Marzook, Ayman B. Farag*, Sudip Kumar Mandal, Syed F. A. Rizvi and Jeetendra Kumar Gupta

Preparation, biological evaluation and radiolabeling of [^{99m}Tc]-technetium tricarbonyl procainamide as a tracer for heart imaging in mice

https://doi.org/10.1515/ract-2021-1079
Received July 16, 2021; accepted January 10, 2022;
published online January 31, 2022

Abstract: This study focuses on the synthesis and preliminary bio-evaluation of [^{99m}Tc]-technetium tricarbonyl procainamide ([^{99m}Tc]-technetium tricarbony PA) as a viable cardiac imaging agent. The compound, [^{99m}Tc]-technetium tricarbony PA, was synthesized by labelling procainamide with a [^{99m}Tc]-technetium tricarbonyl core, yielding a high radiochemical yield and radiochemical purity of 98%. Under optimal circumstances, high radiochemical yield and purity were obtained utilizing [^{99m}Tc]-technetium tricarbonyl core within 30 min of incubation at pH 9, 200 μg substrate concentration, and 100 °C reaction temperature. The heart showed a high absorption of 32.39 ± 0.88% of the injected dose/g organ (ID/g), confirming the suitability of [^{99m}Tc]-technetium tricarbonyl PA as a viable complex for heart imaging.

Keywords: biodistribution; heart imaging; [^{99m}Tc]-tricarbonyl core; [^{99m}Tc]-tricarbonyl procainamide.

1 Introduction

Procainamide (PA), also known as 4-amino-N-[2-(diethylamino)ethyl]benzamide hydrochloride, was chosen therapeutically due to its relationship with sodium channel blockers as an efficient anti-arrhythmic medication useful in the treatment of a wide range of heart conditions (such as atrial and ventricular arrhythmias) [1–9]. Despite the fact that several tracers in the field of heart imaging have been investigated, they all rely on receptors other than sodium channel blockers [6, 10–14]. In addition, some radiotracers worth noting here include [^{99m}Tc]sestamibi, [^{99m}Tc] N-DBODC5, [^{99m}Tc]CO-MIBI, and [^{99m}Tc]tetrofosmin, which are among the most frequently used radiopharmaceuticals for myocardial perfusion imaging. Despite their extensive clinical usage, they are not ideal complexes owing to their high initial hepatic absorption, which might impair interpretation of inferior wall abnormalities due to adjacent photon scatter [15–17]. Therefore, instead of the other receptors previously studied, this tracer, [^{99m}Tc]-technetium tricarbonyl PA, was chosen as a new diagnostic agent that can be utilized in cardiac imaging via sodium channel blocker [15–25]. Nevertheless, there is a key aspect that pertains to the concentration of reported radiotracers in the lungs and heart, as well as blood and liver via β1-receptors. To mitigate the disadvantages, the anti-arrhythmic drug PA was chosen as a potential agent that can be applied in heart imaging via sodium channel blocker rather than the other receptors previously explored. Although PA has previously been labelled with Tc-99m in a previous study, the quantity of complex concentrated in the cardiac muscle was not as significant (i.e., 16.7 ± 0.8% ID/g at 5 min post-injection) [26–43]. Furthermore, as evidenced by its substantial absorption in the stomach (10.5 ± 0.5% ID/g at 120 min post-injection), this chemical is not stable *in vivo*. As a result, further improvements to this molecule, such as the incorporation of a [^{99m}Tc]-tricarbonyl core, are required to improve bio-stability and cardiac absorption while limiting unwanted accumulation in other tissues and/or organs. The aim of this study is to develop the radiotracer, [^{99m}Tc]-technetium tricarbonyl PA (Figure 1), for greater accumulation in cardiac tissues by using a sodium channel blocker, and to investigate the feasibility of the radiotracer as a novel heart-imaging agent [44–50]. Additionally, the biodistribution of

***Corresponding authors: M. H. Sanad**, Labeled Compounds Department, Hot Laboratories Center, Egyptian Atomic Energy Authority, P.O. Box 13759, Cairo, Egypt; and Department of Physics and Engineering Mathematics, Faculty of Engineering, Ain Shams University, P.O. Box 11566, Cairo, Egypt; and **Ayman B. Farag**, Pharmaceutical Chemistry Department, Faculty of Pharmacy, Ahram Canadian University, Giza, Egypt, E-mail: drsanad74@gmail.com (M.H.S), abfarag81@yahoo.com (A.B.F)
Fawzy A. Marzook, Labeled Compounds Department, Hot Laboratories Center, Egyptian Atomic Energy Authority, P.O. Box 13759, Cairo, Egypt
Sudip Kumar Mandal, Department of Pharmaceutical Chemistry, Dr. B. C. Roy College of Pharmacy and Allied Health Sciences, Durgapur 713206, West Bengal, India
Syed F. A. Rizvi, College of Chemistry and Chemical Engineering, Lanzhou University, Lanzhou 730000, Gansu, P. R. China
Jeetendra Kumar Gupta, Institute of Pharmaceutical Research, GLA University Mathura, Uttar Pradesh, India

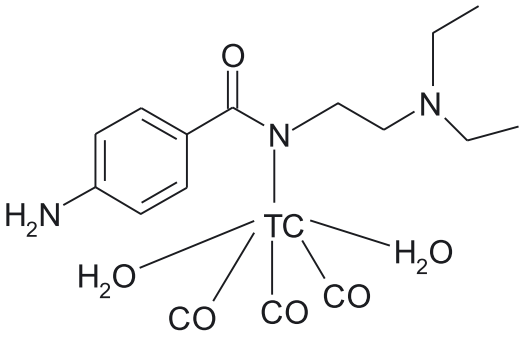

Figure 1: The proposed structure of the molecule, [99mTc]-technetium tricarbonyl PA complex.

the labelled molecule, [99mTc]-technetium tricarbonyl PA, in its target organ (heart) in Swiss Albino mice was explored.

2 Experimental

2.1 General

The drug procainamide (PA) was purchased from Sigma-Aldrich Chemical Company, USA, and all other chemicals and solvents were obtained from Merck Co., Kenilworth, NJ, USA. Thin layer chromatography (TLC) aluminum sheets (20 × 25 cm) SG-60 F_{254} were supplied by Merck. Unless otherwise specified, all chemicals were of analytical grade and were utilized immediately without further purification. Elutec Brussels, Belgium, eluted pertechnetate [$^{99m}TcO_4^-$] from a $^{99}Mo/^{99m}Tc$ generator. For radioactive measurement, a well-type NaI scintillation-counter model Scalar Ratemeter SR7 (Nuclear Enterprises Ltd., USA) was used. Shimadzu reversed-phase HPLC system with a Lichrosorb C-18 column (5 m, 250 × 4.6 mm), an LC-9A pump, a rheodyne injector, interconnected with a UV detector (SPD-6A) for non-radioactive samples and a NaI(Tl) detector for radioactive samples analysis was used. Paper electrophoresis (PE) apparatus from E.C. Corporation (Albany, OR, the United States) was used to observe the charge on the radiopharmaceutical. A gradient mobile phase system consisting of Triethyl ammonium phosphate (TEAP) 0.05 M (solvent A) and methanol (solvent B) was used for the analysis, with a detection wavelength of 254 nm and a flow rate of 0.06 mL min^{-1}. The injection volume of [99mTc]-technetium tricarbonyl PA mixture was 10 µL. The separation was achieved using the gradient program as follows: an isocratic elution (100% A) for the first 0–5 min; linear gradients of 75% A/25% B to 100% A/0% B for 5–8 min; 66% A/34% B to 75% A/25% B for 8–11 min; 0% A/100% B to 66% A/34% B for 11–22 min; and an isocratic elution of 100% B for 22–25 min [26]. Separate fractions of 0.60 mL volume were collected using a fraction collector to a total volume of 25 mL and counted in a well-type NaI(Tl)-counter (BLC-20, BUCK Scientific).

2.2 Radiolabeling

2.2.1 Radiosynthesis of [99mTc]-technetium tricarbonyl precursor: The [99mTc]-technetium tricarbonyl precursor, fac-[[99mTc]-$(CO)_3(H_2O)_3]^+$, was made by adding 1 mL of [99mTc]-pertechnetate ([$^{99m}TcO_4^-$], 750–3500 MBq) to a penicillin vial containing 4.5 mg sodium boranocarbonate, 7.15 mg Na_2CO_3, 8.5 mg sodium tartrate, and 2.85 mg sodium tetra borate [22]. The solution was boiled for 30 min in a boiling water bath, then cooled and adjusted to pH 11. RP-HPLC was used to determine the radiosynthesis yield and stability of the [99mTc]-technetium tricarbonyl precursor by injecting 10 µL of the reaction mixture into the column after filtration with a Millipore filter (0.22 µm).

2.2.2 Radiolabeling procedure of [99mTc]-technetium tricarbonyl PA: Approximately 2 mL of the [99mTc]-technetium tricarbonyl PA radiotracer was radiosynthesized by adding 1 mL of freshly generated [99mTc]-technetium tricarbonyl precursor ion to varied PA concentrations (100–1000 µg, optimum 200 µL PA), 1 mg PA: 1 mL of ethanol, at room temperature, and pH ranges ranging from 3-12 (optimum at pH 9, 200 µL). After that, the reaction vial was heated to 100 °C for 30 min (optimum reaction time) [51–60]. After cooling to room temperature, the radiolabeling yields were measured and validated using thin layer chromatography (TLC) and radio-HPLC.

2.2.3 TLC analysis: The radiochemical conversion to [99mTc]-technetium tricarbonyl PA complex was determined using silica gel GF_{254} plates. Using a non-pointed pencil, the sheets were marked 2 cm above the base with 1 cm lining fragments up to 14 cm. Following filtration with a Millipore filter (0.22 L), 5 µL (1.50 MBq) of the reaction mixture was spotted with a micropipette at lower edge of the plates and allowed to evaporate. The plate was developed using acetonitrile as the mobile phase. The strips were removed, dried, and cut into 1 cm segments, after which the radioactivity was measured using an SR.7 gamma counter [27–29]. The Rf of free [99mTc]-pertechnetate ranged between 0.3 and 0.4. The Rf of [99mTc]-tricarbonyl PA complex was between 0.8 and 1.0, while the Rf of [99mTc]-technetium tricarbonyl precursor was 0.1 [61–77]. The percentage radiolabeling yields of [99mTc]-technetium tricarbonyl PA can then be estimated to yield ≥98%.

2.3 Physicochemical evaluation

2.3.1 Stability in two different media: The stability of [99mTc]-technetium tricarbonyl procainamide complex was determined in two distinct mediums, rat serum and normal saline. In brief, 0.1 mL of purified [99mTc]-technetium tricarbonyl PA complex (3.0×10^{-3} GBq) was added to 1.9 mL of normal rat serum and the mixture was maintained at room temperature for 24 h. Similarly, 0.2 mL of the [99mTc]-technetium tricarbonyl PA complex (3.0×10^{-3} GBq) was added to 0.8 mL of normal saline and incubated for 24 h at room temperature [78–90]. The stability of the radiotracer [99mTc]-technetium tricarbonyl PA complex in two different media was measured using TLC and/or HPLC techniques and counted in a well-type -scintillation counter at different time intervals (at 3, 6, 12, 24, and 48 h).

2.3.2 Biodistribution and animal studies: Animal experiments (using Swiss Albino mice of 35–40 g) were approved by Ethical Committee of the Labeled Compounds Department. Animals were randomly distributed in six groups (n = 5). All animals were intravenously injected with 0.2 mL (200–300 KBq) of [99mTc]-technetium tricarbonyl PA complex via the tail vein. The animals were sacrificed at various time points of post injection (at 5, 15, 30, 60, 120, and 180 min) and

were used to determine the quantitative biodistribution of [^{99m}Tc]-tricarbonyl PA complex in different organs (at each time point). All organs were separated and measured in contrast to a standard solution of the labeled substrate. In addition, fresh blood, bone, and muscle samples were also taken and measured [91–100]. The mean percentage of the administered dose per gram (% ID/g ± SD) was calculated. The blood, bone, and muscle weight ratios were estimated to be 7, 10, and 40% of total body weight, respectively [35, 36]. During the experiments, corrections for background radiation and decay were done. The data were estimated using one way ANOVA test. Results for P were reported and all the outcomes were given as mean ± SD. The P values < 0.05 were considered as statistically significant.

2.3.3 Blocking study: Various concentrations of unlabeled PA as 1 mg PA: 0.15 mL ethanols, 0.15 mL pH 9 at room temperature to give total volume of 0.4 mL of mixture/1 mg PA were used ranging from 0 to 1 mg (0.4 mL of mixture). The study was performed according to the method described in the literature [37–40]. Unlabeled PA, was injected in the range of 0.40 mL (1 mg PA) to 0.10 mL (0.25 mg PA) into the animals 5 min before the administration of the radiotracer, [^{99m}Tc]-technetium tricarbonyl PA complex, and the percentage of cardiac uptake was measured 5 min post injection of the labeled compound [101–110].

3 Results and discussion

3.1 Evaluation of radiolabeling yield by TLC, HPLC, and PE

The radiolabeling yield of [^{99m}Tc]-technetium tricarbonyl procainamide complex compared to free pertechnetate and [^{99m}Tc]-technetium tricarbonyl core was calculated using the percentage (%) on TLC at Rf 0.8 to 1.0, Rf 0.3 to 0.4, and Rf 0.1, respectively. Using a NaI (Tl) γ-ray scintillation counter, an optimal conversion of 98.0% was determined [111–120]. HPLC analysis was used to determine the purity of the [^{99m}Tc]-technetium tricarbonyl PA. As shown in Figure 2A, the R_t values of free [^{99m}Tc]-pertechnetate and [^{99m}Tc]-technetium tricarbonyl core were 11.66 and 4.7 min, respectively. The HPLC chromatogram of reaction mixture revealed two peaks for [^{99m}Tc]-technetium tricarbonyl procainamide complex and [^{99m}Tc]-technetium tricarbonyl core at Rt 9.6 and 4.11 min, respectively (Figure 2B). As shown in Figure 2B, A single and solitary peak (at R_t = 9.6) against the flat background of the HPLC chromatogram revealed the formation of only one complex, [^{99m}Tc]-technetium tricarbonyl procainamide with 99% purity, which can be isolated, evaporated, and then immediately injected into mice. Also, paper electrophoresis was used where [$^{99m}TcO_4^-$], [^{99m}Tc]tricarbonyl core, and [^{99m}Tc]tricarbonyl procainamide moved to different distances away from the spotting point towards the anode (positive electrode) and cathode (negative electrode) to give a distance from spotting point = 11, −2.9, and 0 cm respectively, i.e. this complex has neutral charge.

3.2 Reaction optimization

Many radiolabeling parameters, including reaction duration, substrate quantity (ligand, PA), and pH (acidic-to-basic), were adjusted to achieve 98% radiochemical purity of [^{99m}Tc]-technetium tricarbonyl PA complex [121–129]. Table 1 indicates that when the ligand concentration increased to 200 μg, the conversion to [^{99m}Tc]-technetium tricarbonyl PA complex reached the maximum

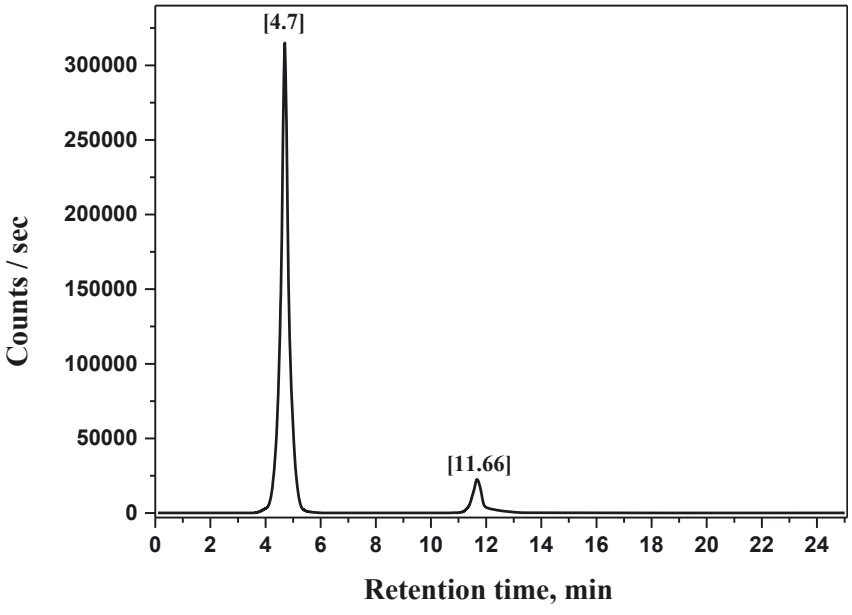

Figure 2A: The HPLC radiochromatogram of [^{99m}Tc]-technetium tricarbonyl precursor, at R_t = 4.7 min and R_t = 11.66 min for free [^{99m}Tc]-pertechnetate.

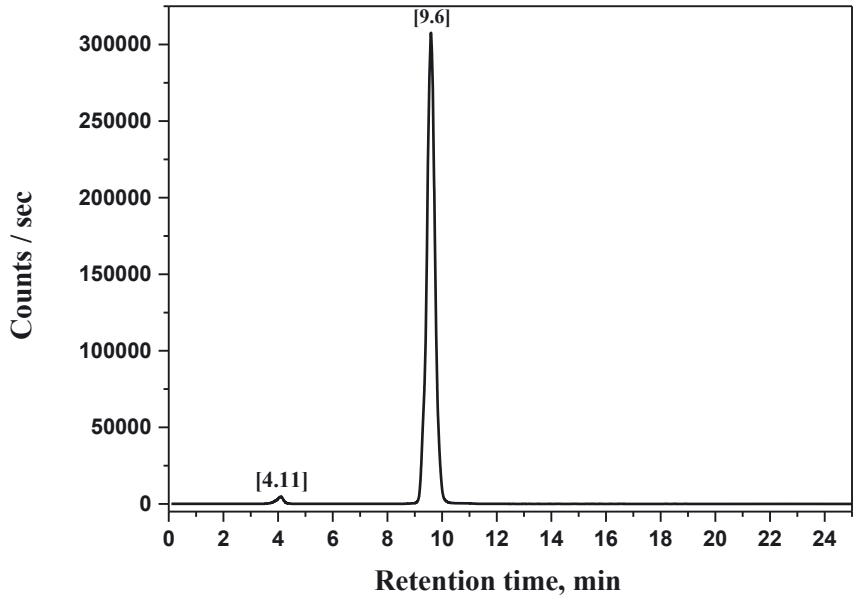

Figure 2B: High performance liquid chromatography (HPLC) analysis. The R_t values of free [99mTc]-technetium tricarbonyl and [99mTc]-technetium tricarbonyl PA complex were 4.11 and 9.6 min, respectively.

Table 1: Effect of changing substrate on radiochemical yield of [99mTc]-technetium tricarbonyl PA complex.

Substrate amount (µg)	[99mTc]-tricarbonyl procainamide	[99mTc]-tricarbonyl precursor
50	55.0 ± 0.19	45.0 ± 0.17
100	70.0 ± 0.16	30.0 ± 0.66
150	88.0 ± 0.20	12.0 ± 0.14
200	98.5 ± 0.15	1.5 ± 0.12
250	98.2 ± 0.14	1.8 ± 0.34
500	95.0 ± 0.18	5.0 ± 0.24
700	94.0 ± 0.98	6.0 ± 0.60
900	93.0 ± 0.16	7.0 ± 0.61

Values represent the mean ± SEM, $n = 3$.

(98.5 ± 0.15%), while the other reaction conditions remained constant. The pH is an important factor influencing the stability of the labelling process, which must also be maintained. The optimal pH was determined to be pH 9, and the radiochemical purity of [99mTc]-technetium tricarbonyl PA complex was 98.5%. As shown in Table 2, the pH value of the reaction mixture below and above 9 has a substantial impact on the optimal radiochemical yield of [99mTc]-technetium tricarbonyl PA complex. In addition, the highest radiochemical yield of [99mTc]-technetium tricarbonyl PA complex was obtained using the optimal reaction duration of 30 min (Table 3). Finally, the stability of

Table 2: Effect of changing pH of reaction mixture on radiochemical yield of [99mTc]-technetium tricarbonyl PA complex.

pH	[99mTc]-tricarbonyl procainamide	[99mTc]-tricarbonyl precursor
3	56.0 ± 0.17	44.0 ± 0.19
4	70.0 ± 0.18	30.0 ± 0.91
5	75.0 ± 0.20	25.0 ± 0.12
7	85.0 ± 0.15	15.0 ± 0.13
8	92.0 ± 0.17	8.0 ± 0.30
9	98.5 ± 0.19	1.5 ± 0.17
10	80.0 ± 0.15	20.0 ± 0.23
12	70.0 ± 0.18	30.0 ± 0.88

Values represent the mean ± SEM, $n = 3$.

Table 3: Effect of reaction time on radiochemical yield of [99mTc]-technetium tricarbonyl PA complex.

Reaction time (minutes)	[99mTc]-tricarbonyl procainamide	[99mTc]-tricarbonyl precursor
1	80.0 ± 0.49	20.0 ± 0.36
15	90.0 ± 0.25	10.0 ± 0.17
30	98.5 ± 0.11	1.5 ± 0.10
45	98.6 ± 0.20	1.4 ± 0.51
60	98.4 ± 0.70	1.6 ± 0.19

Values represent the mean ± SEM, $n = 3$.

Table 4: *In-vitro* stability in rat serum of [99mTc]-technetium tricarbonyl PA complex.

Time (h)	[99mTc]-tricarbonyl procainamide	[99mTc]-tricarbonyl precursor
3	98.6 ± 0.18	1.4 ± 0.55
6	98.3 ± 0.17	1.7 ± 0.61
9	95.0 ± 0.33	5.0 ± 0.48
12	94.0 ± 0.16	6.0 ± 0.12
24	92.0 ± 0.15	8.0 ± 0.39
48	84.0 ± 0.77	16.0 ± 0.29

Values represent the mean ± SEM, $n = 3$.

Table 5: *In-vitro* stability in saline of [^{99m}Tc]-technetium tricarbonyl PA complex.

Time (h)	[^{99m}Tc]-tricarbonyl procainamide	[^{99m}Tc]-tricarbonyl precursor
3	98.5 ± 0.39	1.5 ± 0.98
6	98.6 ± 0.12	1.4 ± 0.78
9	98.4 ± 0.77	1.6 ± 0.93
12	98.0 ± 0.12	2.0 ± 0.17
24	97.0 ± 0.95	8.0 ± 0.38
48	92.0 ± 0.62	8.0 ± 0.81

Values represent the mean ± SEM, $n = 3$.

the [^{99m}Tc]-technetium tricarbonyl PA complex in two distinct mediums was investigated *in vitro* [130–144]. The percentage of radiochemical purity in rat serum was 92% after 24 h and 84% after 48 h (Table 4). The radiochemical purity in saline solution was 97%, and it was shown to be stable for up to 24 h (Table 5).

3.3 Blocking study

Mice were given different doses of PA (0–1 mg/kg) 5 min before receiving the [^{99m}Tc]-technetium tricarbonyl PA complex. At 5 min after injection, the heart uptake dropped from 32.39 to 6% ID/g organ. This is because unlabeled PA binds preferentially to sodium channels in the heart. As a consequence of this study, we can conclude that the compound [^{99m}Tc]-technetium tricarbonyl PA may be successfully used to image sodium channel blockers in the heart of mice (Figure 3) [40].

3.4 Biodistribution study

In normal Swiss Albino mice, a bio-distribution study of the radiotracer [^{99m}Tc]-technetium tricarbonyl procainamide complex was carried out, and the absorption in various organs and fluids is given in Table 6. All levels of radioactivity are expressed as average percent-injected dose per organ (% ID/g organ ± SD) [25–27]. Furthermore, at 5 min post-injection, the radiotracer [^{99m}Tc]-technetium tricarbonyl procainamide was rapidly distributed in most organs such as heart, lungs, liver, intestine, kidneys, heart, stomach, spleen including blood [15]. After 1 h post injection, the uptakes of the liver, intestine, and muscle were 8.55, 5.15, and 4.11%, respectively, and decreased to 2.15, 2.11, and 1.13% at 3 h post injection. In addition, the renal uptake was determined to be 23.9%, at 60 min post infection, and at 3 h post injection, it was reduced to 8.16%. Therefore, the labelled molecule, [^{99m}Tc]-technetium tricarbonyl PA complex, is mostly eliminated through the hepatobiliary and urinary pathways [35]. The stomach uptake was determined to be 1.11% at 5 min post injection and reduced to 0.99% at 3 h post injection, demonstrating the stability of [^{99m}Tc]-technetium tricarbonyl PA complex *in vivo* [22]. At 5 min post injection, the uptake of heart was found to be 32.39%, and at 3 h post injection, it was found to be 5.17%. These findings suggest that the labelled compound, [^{99m}Tc]-technetium tricarbonyl PA complex, has a higher propensity for accumulation than ^{99m}Tc-PA [28]. After 5, 15, 30, 60, 120, and 180 min post injection, the heart-to-liver ratios of the [^{99m}Tc]-technetium tricarbonyl PA complex were 10.87, 7.34, 4.61, 1.68, 1.95, and 2.40%,

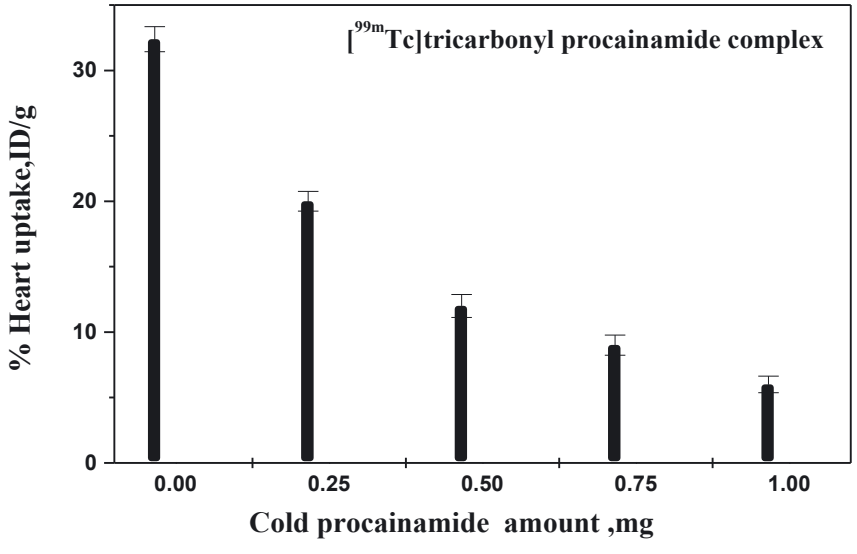

Figure 3: [^{99m}Tc]-technetium tricarbonyl PA complex inhibition heart uptake in normal male Swiss Albino mice at 5 min post injection (%ID/g ± SD, $n = 5$).

Table 6: Biodistribution of [^{99m}Tc]-technetium tricarbonyl PA complex in normal mice at different times.

Organs	% I.D./g at different times post injection					
	5 min	15 min	30 min	60 min	120 min	180 min
Blood	8.77 ± 0.08	4.67 ± 0.11	2.15 ± 0.13	2.12 ± 0.10	1.11 ± 0.20	1.00 ± 0.28
Bone	1.12 ± 0.01	1.10 ± 0.02	0.99 ± 0.00	0.94 ± 0.00	0.91 ± 0.00	0.89 ± 0.00
Muscle	3.17 ± 0.10	3.88 ± 0.02	4.11 ± 0.04	3.16 ± 0.02	2.15 ± 0.02	1.13 ± 0.01
Brain	1.00 ± 0.01	0.98 ± 0.04	0.95 ± 0.01	0.91 ± 0.03	0.89 ± 0.00	0.85 ± 0.00
Lungs	3.11 ± 0.15	2.17 ± 0.05	2.00 ± 0.15	1.19 ± 0.12	1.15 ± 0.13	1.11 ± 0.02
Heart	32.39 ± 0.88	29.14 ± 0.33	25.11 ± 0.44	14.37 ± 0.67	8.12 ± 0.29	5.17 ± 0.19
Liver	2.98 ± 0.11	3.97 ± 0.22	5.44 ± 0.15	8.55 ± 0.52	4.16 ± 0.03	2.15 ± 0.68
Kidneys	4.12 ± 0.13	11.27 ± 0.88	18.67 ± 0.18	23.90 ± 0.11	14.22 ± 0.27	8.16 ± 0.09
Spleen	1.15 ± 0.01	1.10 ± 0.02	1.00 ± 0.01	0.95 ± 0.00	0.90 ± 0.00	0.80 ± 0.00
Intestine	2.12 ± 0.03	3.44 ± 0.16	4.35 ± 0.02	5.15 ± 0.88	4.17 ± 0.08	2.11 ± 0.04
Stomach	1.11 ± 0.10	1.10 ± 0.01	1.00 ± 0.02	0.99 ± 0.01	0.98 ± 0.00	0.99 ± 0.00
Heart/blood	3.70 ± 0.02	6.24 ± 0.09	11.68 ± 0.23	6.78 ± 0.45	7.31 ± 0.31	5.17 ± 0.69
Heart/lungs	10.41 ± 0.52	13.43 ± 0.78	12.56 ± 0.19	12.10 ± 0.77	7.10 ± 0.82	4.66 ± 0.33
Heart/liver	10.87 ± 0.66	7.34 ± 0.73	4.61 ± 0.42	1.68 ± 0.02	1.95 ± 0.02	2.40 ± 0.04

Mean ± SD (mean of five experiments).

respectively (Table 1). Additionally, heart-to-lungs ratios of [^{99m}Tc]-technetium tricarbonyl PA complex was noted to be 10.41, 13.43, 12.56, 12.10, 7.10 and 4.66% at 5, 15, 30, 60, 120 and 180 min post injection, respectively. In comparison to the ^{99m}Tc-PA radiotracer, the [^{99m}Tc]-technetium tricarbonyl PA complex had higher heart-to-liver and heart-to-lungs ratios as reported for heart-to-liver ratios of 2.98, 2.60, 2.40, 2.06, 0.95, and 0.49% at 5, 10, 15, 30, 60, and 120 min post injection, respectively; and heart-to-lungs ratios of 4.63, 4.81, 5.13, 6.38, 5.40, and 3.62% at 5, 10, 15, 30, 60, and 120 min post injection, respectively. In terms of heart-to-liver or lung ratios, the proposed radiotracer [^{99m}Tc]-technetium tricarbonyl PA complex outperformed the ^{99m}Tc-PA complex.

4 Conclusions

An optimized methodology for the synthesis of the radiotracer [^{99m}Tc]-technetium tricarbonyl PA complex with a high radiochemical yield of 98% was established. The stability of the newly synthesized radiotracer was found to be stable (radiolabeling purity of about 98%) in normal saline and rat serum for up to 6 h. The biodistribution studies in mice revealed that [^{99m}Tc]-technetium tricarbonyl PA complex had a high cardiac uptake of 32.39% ID/g at 5 min post injection, which decreased to 5.17% at 3 h post injection. The % ID/g organ values of the [^{99m}Tc]-technetium tricarbonyl PA complex is higher than those of the ^{99m}Tc-PA complex. Therefore, the radiotracer [^{99m}Tc]-technetium tricarbonyl PA complex may be considered a novel cardiac imaging agent.

Author contributions: All the authors have accepted responsibility for the entire content of this submitted manuscript and approved submission.

Research funding: None declared.

Conflict of interest statement: The authors declare no conflicts of interest regarding this article.

References

1. Koch-Weser J., Klein S. W. Procainamide dosage schedules, plasma concentrations, and clinical effects. *J. Am. Med. Assoc.* 1971, *215*, 1454.
2. Bigger J. T., Heissenbuttel R. H. The use of procaineamide and lidocaine in the treatment of cardiac arrhythmias. *Prog. Cardiovasc. Dis.* 1969, *11*, 515.
3. Koch-Weser J. Antiarrhythmic prophylaxis in ambulatory patients with coronary heart disease. *Arch. Intern. Med.* 1972, *129*, 763.
4. Interian A., Zaman L., Velez-Robinson E., Kozlovskis P., Castel-Lanos A., Myerburg R. J. Paired comparisons of efficacy of intravenous and oral procainamide in patients with inducible sustained ventricular tachyarrhythmias. *J. Am. Coll. Cardiol.* 1991, *17*, 1581.
5. Brugada R., Brugada J., Antzelevitch C., Kirsch G. E., Potenza D., Towbin J. A., Brugada P. Sodium channel blockers identify risk for sudden death in patients with ST-segment elevation and right bundle branch block but structurally normal hearts. *Circulation* 2000, *101*, 510.
6. Mian M. S., El-Obeid H. A., Al-Badr A. A. In H. G. Brittain (Ed.), *Analytical Profiles of Drug Substances and Excipients*. Academic Press: California, 26, 1–508, 1999.
7. Mikołajczak R., Garnuszek P. Radiopharmaceuticals in cardiology. *Nucl. Med. Rev. Cent. E Eur.* 2012, *15*, 39.
8. Baggish A. L., Boucher C. A. Radiopharmaceutical agents for myocardial perfusion imaging. *Circulation* 2008, *118*, 1668.

9. Gibbons R. J. Myocardial perfusion imaging. *Heart* 2000, *83*, 355.
10. Jovanović V., Maksin T., Konstantinovska D., Zmbova B., Čvorić J. Radiochemical quality control of ^{99m}Tc-labelled radiopharmaceuticals. *J. Radioanal. Nucl. Chem.* 1980, *59*, 239.
11. Yurt Kilcar A., Biber Muftuler F. Z. Crucial role of radio-chromatography in clinical chemistry of nuclear medicine and radiopharmaceutical research. *Austin Chromatogr.* 2014, *1*, 2.
12. Arano Y. Recent advances in ^{99m}Tc radiopharmaceuticals. *Ann. Nucl. Med.* 2002, *16*, 79.
13. Zolle I. *Technetium-99m Pharmaceuticals: Preparation and Quality Control in Nuclear Medicine*; Springer: New York, 2007.
14. Guo H. X., Zhang J. B., Ma Z., Wang Z. B. Synthesis and biodistribution of ^{99m}TcN-isopentyl xanthate as a potential myocardial perfusion imaging agent. *J. Radioanal. Nucl. Chem.* 2008, *275*, 121.
15. Chen X., Guo Y., Zhang Q., Hao G., Jia H., Liu B. Preparation and biological evaluation of ^{99m}Tc-CO-MIBI as myocardial perfusion imaging agent. *J. Organomet. Chem.* 2008, *693*, 1822.
16. Hatada K., Riou L. M., Ruiz M., Yamamichi Y., Duatti A., Lima R. L., Goode R. A., Watson D. D., Beller G. A., Glover D. K. ^{99m}Tc-N-DBODC5, a new myocardial perfusion imaging agent with rapid liver clearance: comparison with ^{99m}Tc-sestamibi and ^{99m}Tc-tetrofosmin in rats. *J. Nucl. Med.* 2004, *45*, 2095.
17. Hao G. Y., Zang J. Y., Zhu L., Guo Y. Z., Liu B. L. Synthesis, separation and biodistribution of ^{99m}Tc-CO-MIBI complex. *J. Label. Compd. Radiopharm.* 2004, *47*, 513.
18. Sanad M. H., Sallam K. M., Marzook F. A., Abd-Elhaliem S. M. Radioiodination and biological evaluation of candesartan as a tracer for cardiovascular disorder detection. *J. Label. Compd. Radiopharm.* 2016, *59*, 484.
19. Sanad M. H., Ebtisam A. M., Safaa B. C. Radioiodination of olmesartan medoxomil and biological evaluation of the product as a tracer for cardiac imaging. *Radiochim. Acta* 2018, *106*, 329.
20. Ibrahim I. T., Sanad M. H. Radiolabeling and biological evaluation of losartan as a possible cardiac imaging agent. *Radiochemistry* 2013, *55*, 336.
21. Tamer M. S., Sanad M. H., Walaa H. A., Dina H. S., Gehan M. S. Radioiodinated esmolol as a highly selective radiotracer for myocardial perfusion imaging: *in silico* study and preclinical evaluation. *Appl. Radiat. Isot.* 2018, *137*, 41.
22. Safaa B. C., Fawzy A. M., Ayman M. Synthesis of radioiodinated carnosine for hepatotoxicity imaging induced by carbon tetrachloride and its biological assessment in rats. *Radiochim. Acta* 2021, *108*, 397.
23. Massoud A., Challan S. B., Maziad N. Characterization of polyvinylpyrrolidone (PVP) with technetium-99m and its accumulation in mice. *J. Macromol. Sci. A. 58*, 408–418.
24. Mathur A., Mallia M. B., Subramanian S., Banerjee S., Kothari K., Dhotare B., Sarmad H. D., Venkatesh M. 99mTc-N complexes of tertbutyl dithiocarbamate and methoxyisobutyl dithiocarbamate as myocardial and brain imaging agents. *Nucl. Med. Commun* 2005, *26*, 1013.
25. Farid O. M, Ojovan M. I., Massoud A., Shokry S., Rahman R. O. Abdel. An Assessment of Initial Leaching Characteristics of Alkali-Borosilicate Glasses for Nuclear Waste Immobilization. *Mater.* 2019, *12*, 1462.
26. Bissessor N., White H. Valsartan in the treatment of heart failure or left ventricular dysfunction after myocardial infarction. *Vasc. Health Risk Manag.* 2007, *3*, 425.
27. Mohammed El-Sharawy D. M. *Radioiodination and Bioevaluation of Some Cardiovascular Drugs for Nuclear Medicine Application*. Thesis, Department of Pharmaceutics &Industrialpharmacy Faculty of Pharmacy. Cairo University, Egypt, 2013.
28. Massoud A., Mahmoud H. H. Evaluation of hybrid polymeric resin containing nanoparticles of iron oxide for selective separation of In (III) from Ga (III). *J. Inorg. Organomet. Polym* 2017, *27*, 1806.
29. Tejería M. E., Giglio J., Dematteis S., Ana R. A. Development and characterization of a ^{99m}Tc-tricarbonyl–labelled estradiol derivative obtained by "Click Chemistry" with potential application in estrogen receptors imaging. *J. Label. Compd. Radiopharm.* 2017, *60*, 521–527.
30. Kothari K., Joshi S., Venkatesh M., Ramamoorthy N., Pillai M. R. A. Synthesis of ^{99m}Tc$(CO)_3$-mebrofenin via ^{99m}Tc-$[(CO)_3(H_2O)_3]^+$, precursor and comparative pharmacokinetics studies with ^{99m}Tc-mebrofenin. *J. Label. Compd. Radiopharm.* 2003, *46*, 633.
31. Satpati D., Mallia M., Kothari K., Pillai M. R. A. Comparative evaluation of ^{99m}Tc- $[(CO)_3(H_2O)_3]^+$ precursor synthesized by conventional method and by using carbonyl kit. *J. Label. Compd. Radiopharm.* 2004, *47*, 657.
32. He H., Morley J. E., Twamley B., Groeneman R. H., Bucar D. K., MacGillivray L. R., Benny P. D. Investigation of the coordination interactions of S-(pyridin-2-ylmethyl)-L-cysteine ligands with M$(CO)_3$ (M=Re, ^{99m}Tc). *Inorg. Chem.* 2009, *48*, 10625–10634.
33. Jeffrey K., Malgorzata L., Andrew T. T., Luigi G. M. Synthesis and characterization of fac-Re$(CO)_3$-aspartic-Nmonoacetic acid, a structural analogue of a potential new renal tracer, *fac*-^{99m}Tc$(CO)_3$(ASMA). *Eur. J. Inorg. Chem.* 2012, *2012*, 4334.
34. Alberto R., Schibli R., Schubiger A. P. First application of fac $[^{99m}Tc(OH_2)_3(CO)_3]^+$ in bioorganometallic chemistry: design, structure and invitro affinity of a 5-HT1A receptor ligand labeled with ^{99m}Tc. *J. Am. Chem. Soc.* 1999, *121*, 6076.
35. Sanad M. H., El-Bayoumy A. S. A., Ibrahim A. A. Comparative biological evaluation between ^{99m}Tc$(CO)_3$ and ^{99m}Tc-Sn (II) complexes of novel quinoline derivative: a promising infection radiotracer. *J. Radioanal. Nucl. Chem.* 2017, *311*, 1.
36. Malgorzata L., Jeffrey K., Luigi G., Marzilli A., Taylor T. Preclinical evaluation of ^{99m}Tc $(CO)_3$-aspartic-*N*-monoacetic acid, ^{99m}Tc$(CO)_3$(ASMA), a new renal radiotracer with pharmacokinetic properties comparable to ^{131}I-OIH. *J. Nucl. Med.* 2012, *53*, 1277.
37. Sanad M. H., Emad H. B. Comparative biological evaluation between ^{99m}Tc tricarbonyl and ^{99m}Tc-Sn(II) levosalbutamol as a β_2-adrenoceptor agonist. *Radiochim. Acta* 2015, *103*, 879.
38. Rhodes B. A. Considerations in the radiolabeling of albumin. *Semin. Nucl. Med.* 1974, *4*, 281.
39. Hupf H. B., Eldridge J. S., Beaver J. E. Production of iodine-123 for medical applications. *Int. J. Appl. Radiat. Isot.* 1968, *19*, 345.
40. Amin A. M., Sanad M. H., Abd-Elhaliem S. M. Radiochemical and biological characterization of ^{99m}Tc-piracetam for brain imaging. *Radiochemistry* 2013, *55*, 624.
41. Yuan Z., Yue W., Syed F., Askari R., Yida Z., Yintang Z., Xiaoyan L., Haixia Z. Detection of DNA 3′-phosphatase activity based on exonuclease III-assisted cascade recycling amplification reaction. *J. Talanta* 2019, *204*, 499.

42. Siddons C. J. *Metal Ion Complexing Properies of Amide Donating Ligands*. Doctoral Dissertation, University of North Carolina, Wilmington, 2004.
43. Massoud A., Waly S. A., Abou El-Nour F., Removal of U (VI) from simulated liquid waste using synthetic organic resin. *Radiochemistry* 2017, *59*, 272–279.
44. Sanad M. H. Labeling and biological evaluation of 99mTc-azithromycin for infective inflammation diagnosis. *Radiochemistry* 2013, *55*, 539544.
45. Sanad M. H. Labeling of omeprazole with technetium-99m for diagnosis of stomach. *Radiochemistry* 2013, *55*, 605609.
46. Sanad M. H. Novel radiochemical and biological characterization of 99mTc-histamine as a model for brain imaging. *J. Anal. Sci.Technol.* 2014, *5*, 23.
47. Sanad M. H., El-Tawoosy M. Labeling of ursodeoxycholic acid with Technetium-99m for hepatobiliary imaging. *J. Radioanal. Nucl. Chem.* 2013, *298*, 11051109.
48. Sanad M. H., Ibrahim I. T. Radiodiagnosis of peptic ulcer with technetium-99m pantoprazole. *Radiochemistry* 2013, *55*, 341345.
49. Motaleb M. A., Adli A. S. A., El-Tawoosy M., Sanad M. H., AbdAllah M. An easy and effective method for synthesis and radiolabelling of risedronate as a model for bone imaging. *J.Label Compd. Radiopharm.* 2016, *59*, 157163.
50. Sanad M. H., Ibrahim I. T. Radiodiagnosis of peptic ulcer with technetium-99m labeled rabeprazole. *Radiochemistry* 2015, *57*, 425430.
51. Sanad M. H., Salama D. H., Marzook F. A. Radioiodinated famotidine as a new highly selective radiotracer for peptic ulcer disorder detection, diagnostic nuclear imaging and biodistribution. *Radiochim. Acta* 2017, *105*, 389–398.
52. Abdel-Ghaney I. Y., Sanad M. H. Synthesis of ^{99m}Tc-erythromycin complex as a model for infection sites imaging. *Radiochemistry* 2013, *55*, 418–422.
53. Borai E. H., Sanad M. H., Fouzy A. S. M. Optimized chromatographic separation and biological evaluation of ^{99m}Tc-clarithromycin for infective inflammation diagnosis. *Radiochemistry* 2016, *58*, 84–91.
54. Sanad M. H., Challan S. B. Radioiodination and biological evaluation of rabeprazole as a peptic ulcer localization radiotracer. *Radiochemistry* 2017, *59*, 307–312.
55. Sanad M. H., Saleh G. M., Marzook F. A. Radioiodination and biological evaluation of nizatidine as a new highly selective radiotracer for peptic ulcer disorder detection. *J. Label. Compd. Radiopharm.* 2017, *60*, 600–607.
56. El-Kawy O., Sanad M. H., Marzook F. ^{99m}Tc-Mesalamine as potential agent for diagnosis and monitoring of ulcerative colitis: labelling, characterisation and biological evaluation. *J.Radioanal. Nucl. Chem.* 2016, *308*, 279–286.
57. Sanad M. H., Amin A. M. Optimization of labeling conditions and bioevalution of ^{99m}Tc-meloxicam for inflammation imaging. *Radiochemistry* 2013, *55*, 521–526.
58. Sanad M. H., Talaat H. M. Radiodiagnosis of peptic ulcer with technetium-99m-labeled esomeprazole. *Radiochemistry* 2017, *59*, 396–401.
59. Sanad M. H., Alhussein A. I. Preparation and biological evaluation of ^{99m}Tc-N-histamine as a model for brain imaging: in silico study and preclinical evaluation. *Radiochim. Acta* 2018, *106*, 229–238.
60. Sanad M. H., Farouk N., Fouzy A. S. M. Radiocomplexation and bioevaluation of ^{99m}Tc-nitrido-piracetam as a model for brain imaging. *Radiochim. Acta* 2017, *105*, 729–737.
61. Sanad M. H., Sakr T. M., Walaa H. A. A., Marzook E. A. In silico study and biological evaluation of ^{99m}Tc-tricabonyl oxiracetam as a selective imaging probe for AMPA receptors. *J. Radioanal. Nucl.Chem.*, 2017, *314*, 1505–1515.
62. Sanad M. H., Shweeta, H A. Preparation and bio-evaluation of ^{99m}Tc-carbonyl complex of ursodeoxycholic acid for heptobiliary Imaging. *J Mol Imag Dynamic*, 2015, *5*, 1–6.
63. Sanad M. H., Emad H. B. Performance characteristics of biodistribution of ^{99m}Tc-cefprozil for in-vivo infection imaging. *J. Anal. Sci. Technol.* 2014, *5*, 32.
64. Sanad M. H., Abelrahman M. A., Marzook F. M. A. Radioiodination and biological evaluation of levalbuterol as a new selective radiotracer: a β2-adrenoceptor agonist. *Radiochim. Acta* 2016, *104*, 345–353.
65. Sanad M. H., Farag A. B., Dina H. S. J. Radioiodination and bioevaluation of rolipram as a tracer for brain imaging: in silico study, molecular modeling and gamma scintigraphy. *J. Label Compd. Radiopharm.* 2018, *61*, 501–508.
66. Motaleb, M. A., Selim, A. A., El-Tawoosy, M., Sanad M. H., El-Hashash, M. A. Synthesis, radiolabeling and biological distribution of a new dioxime derivative as a potential tumor imaging agent. *J. Radioanal. Nucl. Chem.* 2017, *314*, 1517–1522.
67. Sanad H. M., Ibrahim A. A. Radioiodination, diagnostic nuclear imaging and bioevaluation of olmesartan as a tracer for cardiac imaging. *Radiochim. Acta* 2018, *106*, 843–850.
68. Moustapha, M. E., Motaleb, M. A. & Sanad, M. H. Synthesis and biological evaluation of 99mTc-labetalol for β1-adrenoceptormediated cardiac imaging. *J. Radioanal. Nucl. Chem.* 2016, *309*, 511–516.
69. Sanad M. H., Ibrahim A. A., Talaat H. M. Synthesis, bioevaluation and gamma scintigraphy of ^{99m}Tc-N-2-(Furylmethyl iminodiacetic acid) complex as a new renal radiopharmaceutical. *J. Radioanal. Nucl. Chem.* 2018, *315*, 57–63.
70. Sanad M. H., Fouzy A. S. M., Sobhy H. M., Hathout A. S., Hussain O. A. Tracing the protective activity of Lactobacillus plantarum using technetium-99m-labeled zearalenone for organ toxicity. *Int. J. Radiat. Biol.* 2018, *94*, 1151–1158.
71. Motaleb, M. A., Sanad M. H., Selim, A. A., El-Tawoosy, M., El-Hashash, M. A. Synthesis, characterization, radiolabeling and biodistribution of a novel cyclohexane dioxime derivative as a potential candidate for tumor imaging. *Int. J. Radiat. Biol.* 2018, *94*, 590–596.
72. Sanad M. H., Marzook F. A., Abd-Elhaliem S. M. Radioiodination and biological evaluation of irbesartan as a tracer for cardiac imaging. *Radiochim. Acta* 2021, *109*, 41–46.
73. Sanad M. H., Farag A. B., Saleh G. M. Radiosynthesis and biological evaluation of 188Re-5,10,15,20–Tetra (4-pyridyl)-21H,23H-porphyrin complex as a tumor-targeting agent. *Radiochemistry* 2019, *61*, 347–351.
74. Sanad M. H., Talaat H. M., Fouzy A.S.M. Radioiodination and biological evaluation of mesalamine as a tracer for ulcerative colitis imaging .*Radiochim. Acta*, 2018, *106*, 393–400.
75. Sanad M. H., Sallam K. M., Salama D.H. 99mTc-Oxiracetam as a Potential Agent for Diagnostic Imaging of Brain: Labeling, Characterization, and Biological Evaluation. *Radiochemistry* 2018, *60*, 58–63.

76. Motaleb MA., Sanad M. H. Preparation and quality control of 99mTc-6-{[2-amino- 2-(4-hydroxyphenyl)-acetyl]amino}-3,3-dimethyl- 7-oxo- 4-thia- 1-azabicyclo-heptane- 2-carboxylic acid complex as a model for detecting sites of infection. *Arab Journal of Nuclear Sciences and Applications*, 2012, *45*, 71–77.
77. Sanad M. H., Rizvi F. A., Kumar R. R. Radiosynthesis and bioevaluation of ranitidine as highly selective radiotracer for peptic ulcer disorder detection. *Radiochemistry* 2020, *62*, 119–124.
78. Sanad M. H., Marzook E. A., O. A. El-Kawy O. A. Radiochemical and biological characterization of ^{99m}Tc-Oxiracetam as a model for brain imaging. *Radiochemistry*, 2017, *59*, 624–629.
79. Sanad M. H., Sallam K. M., Marzook F. Labeling and biological evaluation of ^{99m}Tc-tricarbonyl-chenodiol for hepatobiliary imaging. *Radiochemistry* 2017, *59*, 525–529.
80. Sanad M. H., Safaa B. C., Fawzy A. M., Sayed M. A. A., Ebtisam A. M. Radioiodination and biological evaluation of cimetidine as a new highly selective radiotracer for peptic ulcer disorder detection. *Radiochim. Acta* 2021, *109*, 109–117.
81. Sanad M. H., Marzook F. A., Gehan S., Farag A. B., Talaat H. M. Radiolabeling, preparation, and bioevaluation of 99mTc-Azathioprine as a potential targeting agent for solid tumor imaging. *Radiochemistry* 2019, *61*, 478–482.
82. Ibrahim I. T., Abdelhalim S. M., Sanad M. H., Motaleb M. A. Radioiodination of 3-Amino-2-quinoxalinecarbonitrile 1,4-Dioxide and its biological distribution in erhlich ascites cancer bearing mice as a preclinical tumor imaging agent. *Radiochemistry* 2017, *59*, 301–306.
83. Rizvi, S. F. A., Zhang, H., Mehmood, S., Sanad M. H. Synthesis of 99mTc-labeled 2-Mercaptobenzimidazole as a novel radiotracer to diagnose tumor hypoxia. *Translational Oncology* 2020, *13*, 100854.
84. Sanad M. H., Hanan T., Ibrahim I. T., Gehan S., Abozaid L. A. Radioiodinated celiprolol as a new highly selective radiotracer for β1-adrenoceptormyocardial perfusion imaging. *Radiochim. Acta* 2018, *106*, 751–757.
85. Sanad M. H., Eyssa H. M., Gomaa N. M., Marzook F. A., Bassem S. A. Radioiodinated esomeprazole as a model for peptic ulcer localization. *Radiochimica Acta* 2021, *109*, 711–718.
86. Sanad M. H., Rizvi F. A., Kumar R. R., Ibrahim A. A. Synthesis and preliminary biological evaluation of 99mTc-Tricarbonyl ropinirole as a potential brain imaging agent. *Radiochemistry* 2019, *61*, 754–758.
87. Sanad M. H., Rizvi S. F. A., Farag A. B. Synthesis, characterization, and bioevaluation of 99mTc nitrido-oxiracetam as a brain imaging model. *Radiochim. Acta* 2021, *109*, 477–483.
88. Motaleb, M. A., Sanad M. H., Selim, A. A., El-Tawoosy, M., El-Hashash, M. A. Synthesis, characterization, and radiolabeling of heterocyclic bisphosphonate derivative as a potential agent for bone imaging. *Radiochemistry* 2018, *60*, 201–207.
89. Sanad M. H., El-Tawoosy M., Ibrahim I. T. Preparation and biological evaluation of 99mTc-Timonacic acid as a new complex for hepatobiliary imaging. *Radiochemistry* 2017, *59*, 92–97.
90. Sanad M. H., Saad M. M., Fouzy A. S. M., Marzook F., Ibrahim I. T. Radiochemical and biological evaluation of 99mTc-Labeling of phthalic acid using 99mTc-Tricabonyl and 99mTc-Sn (II) as a model for potential hazards imaging. *J Mol Imag Dynamic* 2016, *6*, 1.
91. Sanad, M. H., Ayman F., Dina H. Radioiodination, molecular modelling and biological evaluation of aniracetam as a tracer for brain imaging. *Egypt. J. Rad. Sci. Applic.* 2017, *30*, 131–143.
92. Motaleb M. A., Wanis K. F., Sanad M. H. Synthesis, characterization and labeling of 2-{N, N-dicarboxymethyl (aminoacetyl)} aminothiazole with technetium-99m. *Arab Journal of Nuclear Sciences and Applications* 2005, *38*, 137–145.
93. Motaleb M. A., Wanis K. F., Sanad M. H. Labeling and Biological Distribution of 99mTc-DCMA-AP. *Arab Journal of Nuclear Sciences and Applications* 2006, *39*, 84–91.
94. Sanad M. H., Gizawy M .A., Motaleb M. A., Ibrahim I. T., Saad E. A. A comparative study between stannous chloride and sodium borohydrideas a reducing agents for the radiolabeling of 2,3,7,8,12,13,17,18-octaethyl-21H,23H-porphine with technetium-99m for tumor imaging. *Radiochemistry* 2021, *63*, 507–514.
95. Sanad M. H., Rizvi S. F. A., Farag A. B. Radiosynthesis and in silico bioevaluation of 131I-Sulfasalazine as a highly selective radiotracer for imaging of ulcerative colitis. *Chem Biol Drug Des*., 2021, *98*, 751–761.
96. Sanad M. H., Emam A., Amal S. H., Omaima H., Magdy R., Ahmed F. Distribution of iodine125 labeled parathion and the protective effect of dried banana peel in experimental mice. *Egyptian Journal of Chemistry*, 2022, *65*, 1–2.
97. Sanad H. M., Farag A. B., Motaleb, M. A. Radioiodination and biological evaluation of landiolol as a tracer for myocardial perfusion imaging: preclinical evaluation and diagnostic nuclear imaging. *Radiochim. Acta* 2018, *106*, 1001–1008.
98. Sanad M. H., Rizvi S. F. A., Farag A. B. Design of novel radiotracer 99mTcN-tetrathiocarbamate as SPECT imaging agent: a preclinical study for GFR renal function. *Chemical Papers*, 2022, https://doi.org/10.1007/s11696-021-01926-y.
99. Sanad M. H., Eyssa H. M., Marzook F. A., et al Radiosynthesis and biological evaluation of 99mTc-Nitrido-Levetiracetam as a brain imaging agent. *Radiochemistry*, 2021, *63*, 635–641.
100. Sanad M. H., Eyssa H. M., Marzook F. A.,et al. Comparative bioevaluation of 99mTc-Tricarbonyl and 99mTc-Sn (II) Lansoprazole as a model for peptic ulcer localization. *Radiochemistry*, 2021, *63* , 642–650.
101. Sanad M. H., Marzook F. A., Rizvi S. F. A., Farag A. B., Fouzy A. S. M. *Radioiodinated azilsartan as a new highly selective radiotracer for myocardial perfusion imaging Radiochemistry*, 2021, *63*, 520–525.
102. Sanad M. H., Farag A. B., Marzook F. A., Mandal S. K. Preparation, characterization, and bioevaluation of 99mTc-famotidine as a selective radiotracer for peptic ulcer disorder detection in mice. *Radiochim. Acta*, 2022, https://doi.org/10.1515/ract-2021-1105.
103. Sanad M. H., Farag A. B., Rizvi S. F. A. In silico and in vivo study of radio-iodinated nefiracetam as a radiotracer for brain imaging in mice *Radiochimica Acta*, 2021, *109*, 575–582.
104. EI-Wetery A.S.A., Fayz M. A. A., Sanad M. H., EI-Hashash, M. A. M. Study on the preparation of 99mTc-N-(pyrimidine-2-yl-carbamoyl methyl) iminodiacetic acid as a new complex for hepatobiliary imaging agent. *Arab Journal of Nuclear Sciences and Applications* 2007, *40*, 109–118.
105. Sanad, M. H. , Hanan T., Gehan S. In silico study and preclinical evaluation of radioiodinated procaterol as a potential scintigraphic agent for lung imaging. Egypt. *J. Rad. Sci. Applic.*, 2017, *30*, 117–130.

106. Sanad M. H., Eyssa H. M., Marzook F. A., Rizvi S. F. A., Farag A. B., Fouzy A. S. M., Sabry A. B., Alhussein A. I. Synthesis, radiolabeling, and biological evaluation of 99mTc-Tricarbonyl mesalamine as a potential ulcerative colitis imaging agent. *Radiochemistry* 2021, *63*, 6, 833–840.
107. Sanad M. H., Eyssa H. M., Marzook F. A., Rizvi S. F. A., Farag A. B., Fouzy A. S. M., Mandal S. K., Patnaik S. S. Optimized chromatographic separation and bioevalution of radioiodinated ilaprazole as a new labeled compound for peptic ulcer localization in mice. *Radiochemistry*, 2021, *63*, 6, 811–818.
108. Sanad, M. H. MSc thesis, *Faculty of Science*, Ain-Shams University, Cairo, Egypt, 2007.
109. Sanad, M. H. MSc thesis, *Faculty of Science*, Zagazig University, Cairo, Egypt, 2004.
110. Sanad M. H., Nermien M. G., Nermeen M. E., , Ismail T. I., Ayman M. Radioiodination of balsalazide, bioevaluation and characterization as a highly selective radiotracer for imaging of ulcerative colitis in mice. *J. Label Compd. Radiopharm.* 2022, https://doi.org/10.1002/JLCR.3961.
111. Sanad M. H., Eyssa H. M., Heba M. E. Enhancement of the thermal and physicochemical properties of styrene butadiene rubber composite foam using nanoparticle fillers and electron beam radiation. *Radiochim. Acta*, 2022, https://doi.org/10.1515/ract-2021-1091.
112. Sanad, M. H. *Ulcerative colitis and peptic ulcer imaging* , 1st edn. LAP LAMBERT Academic Publishing, Germany 2017, 1–160.
113. Sanad, M. H. *Nuclear medicine and brain imaging*, 1st edn. LAP LAMBERT Academic Publishing, Germany. 2017, 1–166.
114. Sanad, M. H., Abdel Rahim E. A., Rashed M. M., Fouzy, A. S. M., Omaima A. H., Marzook, F. A., Abd-Elhaliem, S. M. Radioiodination and biological evaluation of parathion as a new radiotracer to study in experimental mice. *World Journal of Pharmacy and Pharmaceutical Sciences* 2020, *9*, 148–158.
115. Ayman F., Ping W., Mahmoud A., Hesham S. *Biological and Medical Chemistry*, 2021, 12003930, https://doi. org/10.26434/chemrxiv.
116. Galal H. E., Nahed M. F., Ayman B., Sheikha A. A. *Nucleosides, Nucleotides and Nucleic Acids*, 2018, *37*, 186–198.
117. Massoud A., Farid O. M., Maree R. M., Allan K. F., Tian Z. R., An improved metal cation capture on polymer with graphene oxide synthesized by gamma radiation. *Reactive and Functional Polymers*, 2020, *151*, 104564.
118. Challan S. B., Massoud A. Radiolabeling of graphene oxide by Tchnetium-99m for infection imaging in rats. *Journal of Radioanalytical and Nuclear Chemistry* 2017, *314*, 2189–2199.
119. Elgemeie G. H., Fathy N. M., Farag A. B.,Yahab I. B. Design and synthesis of new class indeno[1,2-b]pyridine thioglycosides,*Nucleoside & Nucleotide and Nucleic acid*, 2020, *39*, 1–16.
120. Farag A. B.,Ewida H. E., Ahmed M. S., Design, synthesis, and biological evaluation of novel amide and hydrazide based thioether analogs targeting Histone deacteylase (HDAC) enzymes, *European journal of medicinal chemistry*, 2018, *148*, 73–85.
121. Elgemeie G. H., Fathy N. M., Farag A. B.,Kursani S. A.Design, synthesis, molecular docking and anti-hepatocellular carcinoma evaluation of novel acyclic pyridine thioglycosides, *Nucleoside & Nucleotide and Nucleic acid* 2018, *37*, 186–198.
122. Farag A. B., Magdi A., Spectrophotometric study of the interaction between a novel benzothiazolethioglycoside as antimicrobial agent with bovine serum albumin, *Chemistry Research Journal*, 2017, *2*, 66–72.
123. Elgemeie G. H., Farag A. B.,Design, synthesis, and in vitro anti-hepatocellular carcinoma of novel thymine thioglycoside analogs as new antimetabolic agents, *Nucleoside & Nucleotide and Nucleic acid.*, 2017, *36*, 328–342.
124. Elgemeie G. H., Fathy N. M., Farag A. B., Kursani S. A.Novel synthesis of dihydropyridine thioglycosides and their cyctotoxic activity, *Nucleoside & Nucleotide and Nucleic acid.*, 2017, *36*, 355–377.
125. Elgemeie G. H., Fathy N. M., Zaghary W. A., Farag A. B., S-Glycosides in Medicinal Chemistry: Novel Synthesis of CyanoethyleneThioglycosides and Their Pyrazole Derivatives, *Nucleoside & Nucleotide and Nucleic acid*, 2017, *36*, 198–212.
126. Farag A. B., Wang P., Boys I., Schoggins J., Sadek H., Identification of Atovaquone, *Ouabain and Mebendazole as FDA Approved drugs targeting SARS-COV-2*, ChemRxiv, 2020.
127. White R. L., White C. M., Turgut H., Massoud A., Tian Z. R., Comparative studies on copper adsorption by graphene oxide and functionalized graphene oxide nanoparticles, *J Taiwan Inst Chem Eng* 2018, *85*, 18–28.
128. Bekheet S., El-Tawoosy M., Massoud A., Borei I. H., Ghanem H. M., ^{99m}Tc-labeled ceftazidime and biological evaluation in experimental animals for detection of bacterial infection. *Am. J. Biochem* 2014, *4*,15–24.
129. Massoud A., Rizk H. E., Attallah M. F., Selective separation of Y(III) from Sr(II) using hybrid polymer: synthesis, characterization, batch and column study, *Polym. Bull.* 2021, *78*, 7053–7069.
130. Zaky M. M., Eyssa H. M., Sadek R. F. Improvement of the magnesium battery electrolyte properties through gamma irradiation of nano polymer electrolytes doped with magnesium oxide nanoparticles. *J. Vinyl Addit. Technol.* 2019, *25*, 243.
131. Senna M. M., Youssef H. A., Eyssa H. M. Effect of electron beam irradiation, EPDM and azodicarbonamide on the foam properties of LDPE sheet. *Polym. Plast. Technol. Eng.* 2007, *46*, 1093.
132. Eyssa H. M., El Mogy S. A., Youssef H. A. Impact of foaming agent and nanoparticle fillers on the properties of irradiated rubber. *Radiochim. Acta* 2021, *109*, 127.
133. Hegazi E. M., Eyssa H. M., Abd El-Megeed A. A. Effect of nanofiller on the ageing of rubber seal materials under gamma irradiation. *J. Compos. Mater.* 2019, *53*, 2065.
134. Eyssa H. M., Osman M., Kandil S. A., Abdelrahman M. M. Effect of ion and electron beam irradiation on surface morphology and optical properties of PVA. *Nucl. Sci. Tech.* 2015, *26*, 060306.
135. Eyssa H. M., Elnaggar M. Y., Zaky M. M. Impact of graphene oxide nanoparticles and carbon black on the gamma radiation sensitization of acrylonitrile–butadiene rubber seal materials. *Polym. Eng. Sci.* 2021, *61*, 2843.
136. Youssef H. A., Senna M. M., Eyssa H. M., Sarhan A. Fabrication of sponge nitrile butadiene rubber (NBR) by subsequent sulphur and electron beam irradiation. *Mans. J. Chem.* 2010, *37*, 155.
137. Senna M. M., Mostafa A. B., Mahdy S. R., El-Naggar A. M. Characterization of blend hydrogels based on plasticized starch/ cellulose acetate/carboxymethyl cellulose synthesized by electron beam irradiation. *Nucl. Instrum. Methods Phys. Res. B* 2016, *386*, 22–29.
138. Eyssa H. M., Sawires S. G., Senna M. M. Gamma irradiation of polyethylene nanocomposites for food packaging applications

against stored-product insect pests. *J. Vinyl Addit. Technol.* 2019, *25*, 120.
139. Eyssa H. M., Abulyazied D. E., Abo-State M. A. M. Application of polyurethane /gamma-irradiated carbon nanotubes composites as antifouling coat. *Polym. Compos.* 2018, *39*, E1196.
140. Eyssa H. M., Mohamed W. S., El-Zayat M. M. Irradiated rubber composite with nano and microfillers for mining rock application. *Radiochim. Acta.* 2019, *107*, 737.
141. Youssef A. H., Senna M. M., Eyssa H. M. Characterization of LDPE and LDPE/EVA blends crosslinked by electron beamirradiation and foamed with chemical foaming agent. *J. Polym. Res.* 2007, *14*, 351.
142. Eyssa H. M., Abulyazied D. E., Abdulrahman M., Youssef H. A. Mechanical and physical properties of nanosilica/nitrile butadienerubber composites cured by gamma irradiation. *Egypt. J. Petro.* 2018, *27*, 383.
143. Youssef H. A., Abdel-Monem Y. K., El-Sherbiny I. M., Eyssa H. M., El-Raheem H. M. Effect of ionizing radiation on the properties ofsome synthesized polyurethanes. *J. Pharm. Biol. Chem. Sci.* 2016, *7*, 855.
144. Eyssa H. M., Hassan M. S. Surface characteristics of cotton/ polyester fabric coated with poly-urethane elastomers cured thermally or by using gamma irradiation. Egypt. *J. Rad. Sci. Applic.* 2014, *27*, 91.